Cleaner Logistics and Supply Chain 9 (2023) 100130

Contents lists available at ScienceDirect

Cleaner Logistics and Supply Chain

journal homepage: www.journals.elsevier.com/cleaner-logistics-and-supply-chain

Global warming potential of lithium-ion battery cell production: Determining influential primary and secondary raw material supply routes

Mohammad Abdelbaky [a,b,*], Lilian Schwich [c,d], João Henriques [a,b], Bernd Friedrich [d], Jef R. Peeters [a,b], Wim Dewulf [a]

[a] KU Leuven, Department of Mechanical Engineering, Celestijnenlaan 300, 3001 Leuven, Belgium
[b] Core Lab E2E, Flanders Make, 3000 Leuven, Belgium
[c] Cylib GmbH, Philipsstr. 8, D-52068 Aachen, Germany
[d] IME Process Metallurgy and Metal Recycling, RWTH Aachen University, D-52056 Aachen, Germany

ARTICLE INFO

Keywords:
Lithium-ion battery recycling
Critical raw materials
Life cycle assessment
Sensitivity analysis

ABSTRACT

This study assesses the global warming potential (GWP) impacts of lithium-ion battery (LIB) recycling and subsequent cell production from primary and secondary raw materials. Furthermore, the study proposes multiple allocation strategies for the GWP impacts of LIB recycling, which range from 18 to 22 kg CO_2 equivalent per kilowatt-hour NMC111 and NMC811 battery packs to determine the environmental burdens of secondary raw materials. The results demonstrate that using secondary raw materials could ideally reduce NMC111 and NMC811 cell production GWP by 30 %. In practice, GWP impact reductions will vary depending on factors, such as the contributions of primary production and recycling to battery raw material supply, and the market share of the different technologies employed within both primary production and recycling.

Based on estimates for the availability of recycled raw materials to the European battery value chain, the sensitivity analysis methods identified NMC hydroxide, nickel sulfate, and battery-grade graphite as the most influential recycled raw materials on NMC111 cell production GWP. These materials received importance scores of 59%, 8%, and 6% respectively. Primary supply routes for cobalt sulfate received the highest importance score, followed by the primary supply routes of lithium carbonate and nickel sulfate. For NMC811 cells, nickel sulfate (34%), NMC hydroxide (27%) and graphite (8%) were identified as the most influential recycled raw materials, with the primary supply routes of nickel sulfate, lithium hydroxide and battery-grade graphite being the most influential.

1. Introduction

The European Commission (EC) is committed to having zero greenhouse gas (GHG) emissions from new vehicles by 2035 to achieve climate neutrality (European Commission, 2019). Despite only accounting for 14 % of global car sales in 2022 (IEA, 2023), plug-in hybrid and battery electric vehicles (EVs) – the most prominent low and zero-emission vehicle technologies – have already become the largest end-use sector for LIBs (Pillot, 2021). Therefore, the production of LIBs is deemed a key factor in this transition. Furthermore, the EC launched the European Battery Alliance to create a sustainable and competitive European battery value chain (European Commission, 2021).

Currently, raw materials account for 70 % of LIB cell production costs (Moores, 2022), and the EU heavily relies on third countries for the supply of many of these materials. Recognizing these dependencies, the EC has taken steps to address them through the Critical Raw Materials Act (European Commission, 2023). The vulnerability of this reliance is evident in recent LIB price fluctuations. Despite expectations of declining prices due to increased production scale (Goldie-Scot, 2019; IEA, 2019), the cost of LIB cells in 2022 increased by 20 % compared to 2019 (Shah, 2022). These price increases were initially triggered by the COVID-19 pandemic, and are now being further driven by demand for EVs in China and the Russian-Ukrainian conflict, amid fears of battery-grade nickel (Ni) and aluminum (Al) supply disruptions (Jin, 2022; IEA, 2023).

The significance of raw materials in LIB production extends beyond supply challenges, as research has shown that GHG emissions from LIB production are largely influenced by cathode materials, which, in turn,

* Corresponding author at: Celestijnenlaan 300, BOX 2422, 3001 Leuven, Belgium.
E-mail address: mohammad.abdelbaky@kuleuven.be (M. Abdelbaky).

https://doi.org/10.1016/j.clscn.2023.100130
Received 12 August 2023; Received in revised form 27 November 2023; Accepted 30 November 2023
Available online 6 December 2023

are influenced by the mining and extraction processes associated with raw material production (Lai et al., 2022). Furthermore, the new EU battery regulation requires EV batteries to contain at least 12 % recycled lithium (Li) content, 15 % Ni, and 26 % cobalt (Co) by 2036 (European Parliament, 2023). This can be an effective measure for reducing resource consumption and GHG emissions from LIB cell production in the short term (Qiao et al., 2019; Tytgat, 2022; Chen et al., 2022). Additionally, end-of-life EV batteries can be a strategic resource of battery raw materials due to their high concentrations of Li, Co, and Ni, which can be 5 to 17 times higher than the respective natural ores (Lovins, 2022).

Previous research on the life cycle assessment (LCA) of LIB hydrometallurgical recycling estimated GWP savings in recycling to be 38 %, compared to the virgin production of rare earths, Li, Ni, and Co (Rinne et al., 2021). The study by Blömeke et al. (2022) further confirmed these findings while also emphasizing that other recycling routes, including pyrometallurgical and hybrid processes, can potentially reduce the environmental impacts associated with battery raw material production (Blömeke et al., 2022). However, it is unlikely that Europe will be able to close the circularity gap in the coming decennium for battery raw materials (Abdelbaky et al., 2021). Therefore, commercial primary production and LIB recycling processes will play a vital role in feeding battery raw materials in the near to mid future.

Despite the significant influence of raw materials on LIB production and their potential for reducing GWP, the existing body of LCA studies predominantly focused on other aspects such as cell design, battery specific energy, energy consumption during the manufacturing process, and the electricity mix used (Bouter & Guichet, 2022). Similarly, (Porzio & Scown, 2021) concluded that previous LCA studies have not thoroughly investigated the influence of average and marginal sources of key raw materials. However, a more recent study by (Xu et al., 2022) modelled the production of eight LIB cell chemistries using background life cycle inventory (LCI) data that consider future energy scenarios and supply chains of key battery metals. The authors concluded that cell chemistries such as lithium iron phosphate should be widely deployed due to their low GHG emissions, as well as using low-carbon electricity supply in cell production. However, this study used averaged LCIs for primary Ni and Co production, and did not include either electrolytic manganese (Mn) production routes or secondary raw materials. A second study by (Pell & Lindsay, 2022) on the life cycle impacts of solid-state and conventional LIBs concluded that graphite produced in China significantly contributes to the environmental impacts, and recycled battery raw materials may provide an additional source of avoided impacts. However, the study applied a local sensitivity analysis, which limited the examination of the influence of market share among different primary supply routes. Additionally, recycled raw materials were excluded from their analysis. A third study by (Manjong et al., 2021) presented extensively parameterized LCIs for battery raw materials' extraction and refining. However, the significance of parameters such as ore grade decline and metal extraction rate from ores during the smelting process on LIB cell production GWP was not evaluated because of the scope of the study.

As nuances in the market share of different primary and secondary supply routes were not sufficiently examined in the literature, the present study aims to address this gap by quantifying the magnitude of change in environmental impacts at the cell level, taking into account these supply chain intricacies. Therefore, a comprehensive methodology is presented that includes three steps:

1) Primary and secondary supply routes for Li, Ni, Co, Mn, and graphite are aggregated on LIB cell level in parameterized LCIs, and cell chemistries with cathode materials $LiNi_{1/3}Mn_{1/3}Co_{1/3}O_2$ (NMC111) and $LiNi_{8/10}Mn_{1/10}Co_{1/10}O_2$ (NMC811) are selected as reference chemistries. It is noteworthy that these five raw materials have been designated as strategic raw materials according to the proposed amendment to the European Critical Raw Materials Act by the EC (European Commission, 2023).
2) LCA is performed to evaluate the GWP impacts of LIB cell production and estimate the variability due to a diverse raw material supply from primary and secondary production.
3) Global sensitivity analysis methods are applied to mathematically determine and rank the most influential primary and secondary supply routes on cell production GWP impacts.

This methodology aims to provide a deeper understanding of the environmental impact of primary production and secondary supply of LIB raw materials by taking into account state-of-the-art and market-driven primary supply routes, as well as closed-loop pyro- and hydrometallurgical recycling of LIBs.

2. Methods

2.1. Assessing GWP impacts of LIB cell production

The goal of the LCA study is to examine GWP impacts from the production of 1 kilowatt-hour (kWh) LIB cells, which is equivalent to 5.1 and 4.8 kg NMC111 and NMC811 cells, respectively (Crenna et al., 2021). The study aims to identify the extent at which primary and secondary raw material supply routes influence cell production GWP. The NMC111 and NMC811 cell chemistries are selected as references for the study because NMC111 cells, on the one hand, dominated new EV sales in Europe until 2015 and will have a considerable share in the emerging recycling waste stream. On the other hand, NMC811 cells are expected to be widely adopted in the near future (Abdelbaky et al., 2021; IEA, 2023). Therefore, the study can also determine the effect of evolving technologies on both production and closed-loop recycling.

The scope of the study further includes the recycling of EV batteries, as it is expected to be a significant source of recycled LIB raw materials. The objective is to assess the environmental burdens of feedstock from LIB recycling and to evaluate the sustainability of different recycling methods compared to the current market-driven primary supply routes. Furthermore, the study seeks to explore how advancements in LIB recycling can contribute to a more sustainable battery value chain. The assessment of GWP impacts is carried out using the 100-year climate change baseline model of the IPCC 2013 as implemented in the EF v3.0 method (Fazio et al., 2018) and calculations are performed with the open source LCA software, Activity Browser (Steubing et al., 2020).

In this study, cell production is modelled twice, once with recycled raw materials sourced entirely from pyrometallurgical recycling and once from hydrometallurgical recycling. The LCIs for the production of LIB cells are created using a parametric approach, as illustrated in Fig. 1. The first set of parameters relates to the share and type of recycled raw materials used in LIB cell production. To determine this, estimates are used for the closed-loop recycling potential for fulfilling sectoral raw material demand from the study by (Abdelbaky et al., 2021), specifically the results from the baseline sales scenario in 2040. The use of the 2040 recycling potential is chosen as it represents the maximum potential for closed-loop recycling, taking into account the expected exponential growth in EV sales, extended battery life in vehicle use, and potential for second use. The second set of parameters relates to the primary supply routes for battery-grade raw materials whose values are estimated based on literature studies, market outlooks, and expert opinions.

2.2. Primary supply routes considered in this study

2.2.1. Lithium

Li is extracted from three main sources; spodumene pegmatite rocks, evaporative brines, and unusual deposits from both rocks and brines (Kesler et al., 2012). Furthermore, more than 90 % of global mine production is from mine operations in Argentina, Australia, Brazil, Chile, and China, which extract Li from brine and spodumene sources

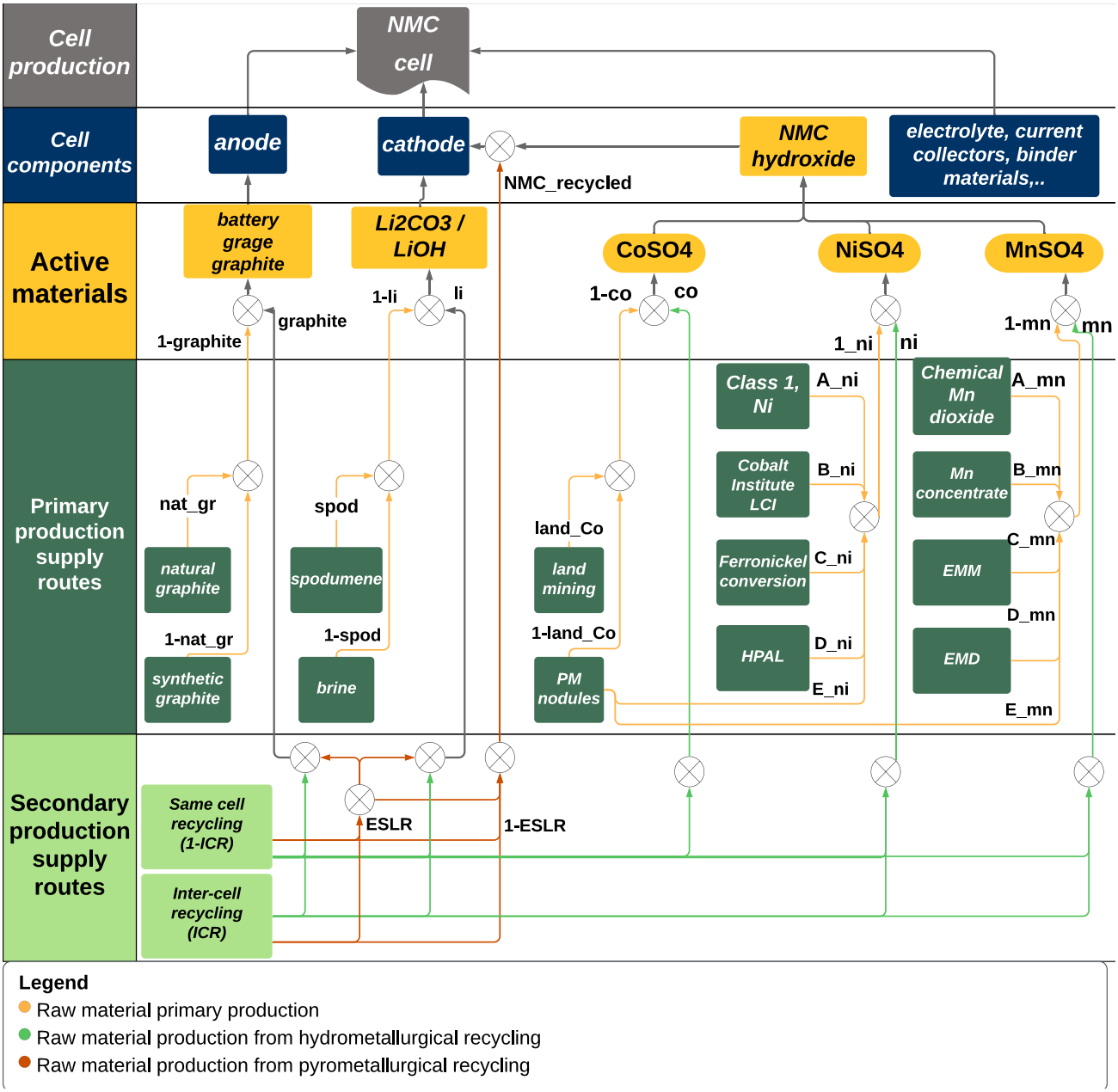

Fig. 1. Visual representation of the parameterized cell production LCI and parameter insertion.

(U.S. Geological Survey, 2023). Therefore, this study uses the LCIs for lithium carbonate (Li_2CO_3) and lithium hydroxide (LiOH) production from spodumene rocks (Jiang et al., 2020) and brines (Stamp et al., 2012) as implemented in the Ecoinvent 3.8 database (Wernet et al., 2016) to evaluate the GWP impact of Li content in LIBs.

2.2.2. Nickel

Ni is the battery raw material with the least available reserves and highest reserves depletion rate (Abdelbaky et al., 2022). In addition to production from sulfide ores, it is forecasted that a significant share of future battery-grade nickel sulfate ($NiSO_4$) supply will come from laterite ore processing routes, such as nickel pig iron/ferronickel conversion and high-pressure acid leaching (HPAL), due to the large projects under construction in Indonesia (Lennon, 2021). Another potential source of future Ni supply are deep-sea polymetallic (PM) nodules. According to (Morgan, 2017), PM nodules in the Clarion-Clipperton zone in the North Pacific contain roughly 9 billion tons of strategic battery raw materials, including Mn, Ni, Co, and copper (Cu).

LCIs for $NiSO_4$ production from primary company data sources, such as those published by the Nickel (Sphera, 2021) and Cobalt Institutes (Cobalt Institute, 2016), are deemed unsuitable on their own as they average data from multiple conversion routes. However, this study aims to isolate and scrutinize the effects of high and low CO_2 emission routes based on their potential market share in the future. Hence, this study adopted an alternative approach, relying on LCIs derived from literature studies to comprehensively examine the influence of $NiSO_4$ primary production. First, $NiSO_4$ primary supply routes in the Ecoinvent 3.8 database are considered; i.e. from class I Nickel and the Cobalt Institute's aggregated LCI (Arvidsson et al., 2022). Second, this study presents two LCIs for $NiSO_4$ supply from ferronickel conversion and HPAL that are representative of high CO_2 emission laterite ore processing routes (supporting information S1). Finally, this study includes the LCI of $NiSO_4$ production from PM nodules that was published in the study of (Paulikas et al., 2020) as a representative route for

unconventional low CO_2 emission production.

2.2.3. Cobalt

Today, co-production of Co from Ni and Cu ores accounts for 95 % of mine supply (Abdelbaky et al., 2022). Therefore, this study considers the industry average cradle-to-gate LCI for cobalt sulfate ($CoSO_4$) production from the LCA study commissioned by the Cobalt institute (Cobalt Institute, 2016), and as implemented in the Ecoinvent database. In addition, this study considers the LCI for $CoSO_4$ from PM nodules from the study by (Paulikas et al., 2020) to represent unconventional low CO_2 emission production (supporting information S1).

2.2.4. Manganese

Primary and secondary batteries use one of three main groups of manganese dioxides: natural, chemical, and electrolytic (Önal et al., 2021). The Ecoinvent database models manganese sulfate ($MnSO_4$) production for LIBs from manganese concentrate, and as a byproduct of manganese dioxide production (GLAD, 2020). However, (Paulikas et al., 2020) criticized these datasets for leaving out major refining steps and material inputs needed to produce battery-grade $MnSO_4$, stating that the LCI data can only serve as an "extreme lower bound". Therefore, this study incorporates three additional LCIs for the primary production of $MnSO_4$ from electrolytic manganese metal (EMM), electrolytic manganese dioxide (EMD), and PM nodules (supporting information S1), which complement the Ecoinvent datasets for $MnSO_4$ production. The EMM and EMD supply routes are becoming the preferred starting raw material for producing high purity $MnSO_4$ because China, the world's largest LIB cell manufacturer, has 98 % of global EMM production capacity (Boubou, 2018; Zhang et al., 2020). Additionally, PM nodules are a potential source of future Mn supply and are selected to represent unconventional less CO_2 emitting supply routes (Paulikas et al., 2020).

2.2.5. Graphite

Battery-grade graphite can be produced from natural ore deposits (termed natural graphite) or synthetic sources such as coal tar and petroleum coke (termed synthetic graphite) (Tsuji, 2022). This study will consider two supply routes for battery-grade graphite from natural and synthetic routes. The LCI inventory of natural graphite production from the study of (Engels et al., 2022a) will be used instead of the one in Ecoinvent database because of the high uncertainty and poor data quality (Engels et al., 2022b). For the synthetic route, this study relies on the LCI from the work of (Dunn et al., 2015) as implemented in the Ecoinvent database.

2.3. Secondary supply routes considered in this study

2.3.1. Hydrometallurgy: solvent extraction

The LCI for solvent-based extraction of important battery raw materials from waste LIBs is developed based on the study of (Rinne et al., 2021) and is illustrated in Fig. 2A. The LCI is adapted to specifically model the recycling of LIBs, instead of the synergistic recycling of LIBs and nickel metal hydride batteries, as detailed in the supporting information S2. In the developed LCI, it is considered that, prior to acid leaching and solvent-based extraction of battery raw materials, the black mass is treated by flotation to recover graphite. Graphite flotation is an effective separation strategy due to the different hydrophobic and hydrophilic behaviors of anode and cathode material (Zhang et al., 2019a). The flotation process has the advantage of avoiding excess acid consumption and difficult separation of residues from leaching solution (Zhang et al., 2019b). A study by (Zhang et al., 2018) demonstrates that recycled graphite can be regenerated by coating with pyrolytic carbon from phenolic resin. Therefore, this method has been included in the LCI of this recycling process. As such, the following battery raw materials

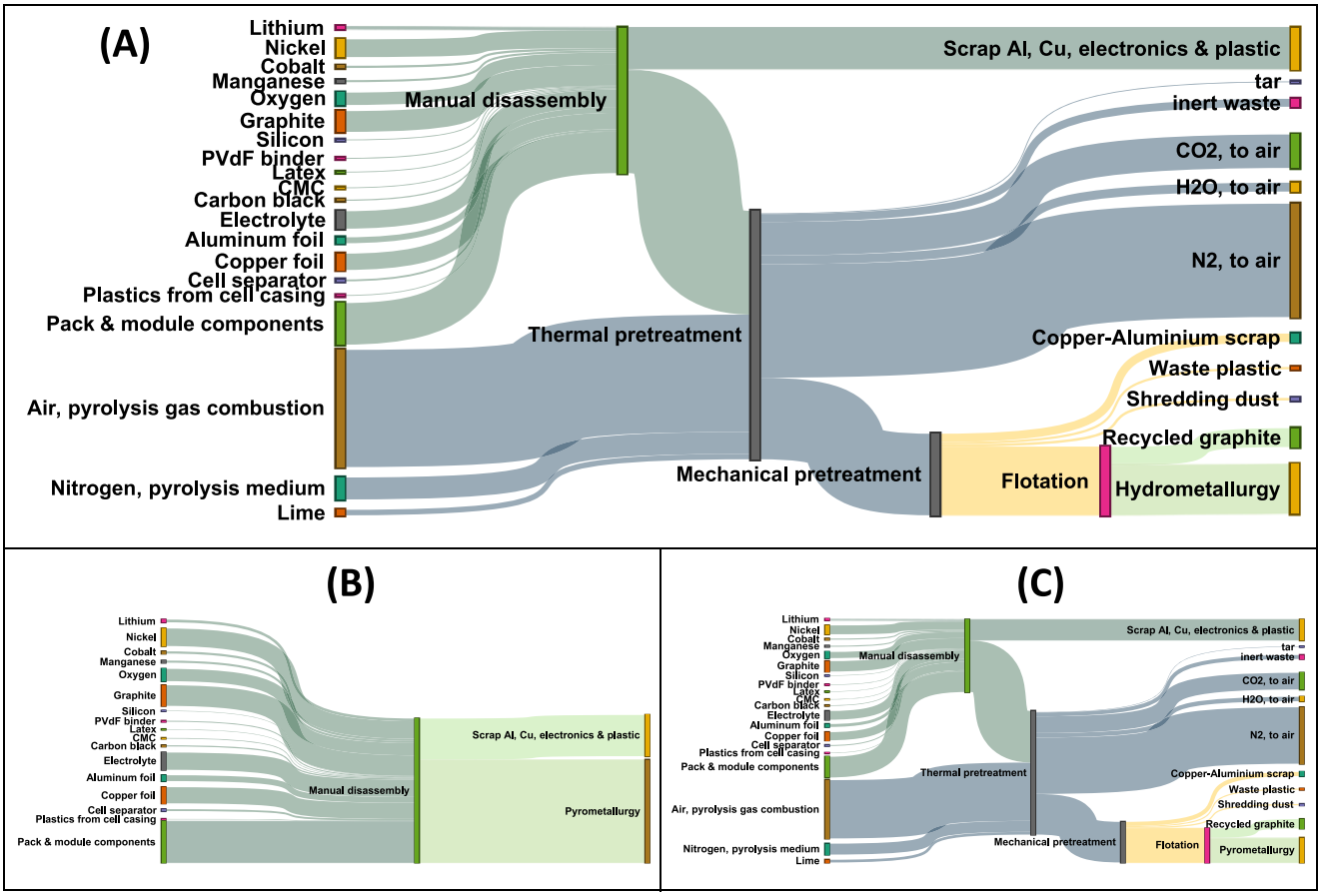

Fig. 2. Sankey Diagram of Recycling Processes for NMC811 Battery Pack (A) Hydrometallurgy, (B) Conventional Pyrometallurgy, (C) Enhanced Pyrometallurgy.

are recovered in this hydrometallurgical recycling process:

- Al from the battery pack housing or embodiment
- Cu current collector foils from the mechanical pretreatment step
- Graphite is recovered in the flotation process
- Mn is recovered as manganese dioxide using potassium permanganate ($KMnO_4$), which is then converted to $MnSO_4$ in an ion-exchange reaction
- Ni is recovered as $NiSO_4$ by solvent based extraction
- Co is recovered as $CoSO_4$ by solvent based extraction
- Li is recovered as Li_2CO_3 by precipitation with soda ash (Na_2CO_3)

Al recycling is mostly done mechanically, with only a small percentage subjected to hydrometallurgy. Because of the low efficiency of this process, Al from the cell casing and current collectors is assumed to be diluted in the copper foil fraction or precipitated as waste in the solvent extraction step. Future advancements in sorting technologies can potentially improve Al recovery in hydrometallurgical recycling processes.

The advantage of this solvent extraction process is that Ni, Co, and Mn are recovered as separate products, which makes it easy to adjust their molar ratios in the production of NMC hydroxides for new LIB cells. Additionally, the study provides new LCIs, in supporting information S3, for the chemicals and solvents used in battery recycling based on literature studies and the modelling approach proposed by (Hischier et al., 2004). Recycled feedstock from this process is included in the LCI of cell production using parameters "li", "ni", "co", "mn" and "graphite". These parameters correspond to cell content of recycled Li_2CO_3/LiOH, $NiSO_4$, $CoSO_4$, $MnSO_4$, and graphite.

2.3.2. Pyrometallurgical recycling

This study considers both a conventional process and an enhanced process to represent the pyrometallurgical recycling of LIBs. The LCI for conventional pyrometallurgical recycling of waste LIBs is developed based on energy consumption estimates from the work of (Dai et al., 2019) and (George et al., 2006), as presented in Fig. 2B. The metals contained in waste LIBs are separated according to their oxygen affinity (Windisch-Kern et al., 2021), which presents a challenge for the recycling method depicted in Fig. 1B. On the one hand, Li has a high affinity for oxygen and is therefore fixed in the solid slag, while graphite in the anode powder is burnt and not recovered (Zhang et al., 2019b; Ma et al., 2019). On the other hand, metals with low oxygen affinity, such as Ni and Co, are recovered together as an alloy known as "matte." In a subsequent process, the Ni-Co-Cu matte is refined to produce copper sulfate ($CuSO_4$) and an NMC hydroxide product by co-precipitation of Ni, Co, and Mn with sodium hydroxide (NaOH). Recycled feedstock from this process is included in the LCI of cell production using parameters "NMC111" or "NMC811". These parameters correspond to cell content of recycled NMC111/NMC811 hydroxide.

The enhanced pyrometallurgical recycling process is illustrated in Fig. 2C. Although this process has more preprocessing steps than the conventional one, yet it has the advantage of recovering Li and graphite prior to black mass smelting. In a first step, early-stage lithium recovery involves mobilizing Li from the black mass by supercritical CO_2 carbonation (Schwich et al., 2021). In a second step, graphite is recovered by flotation. In this enhanced pyrometallurgical recycling process, the following battery raw materials are recovered:

- Al from the battery pack jacket
- Cu foils from the mechanical pretreatment step
- Li is recovered as Li_2CO_3 by supercritical CO_2 carbonation
- Graphite is recovered in the flotation process
- Remaining Cu in black mass is recovered as $CuSO_4$ by solvent based extraction
- Ni, Co, & Mn are recovered as an NMC hydroxide by coprecipitation

Recycled feedstock from this process is included in the LCI of cell production using parameters "li", "graphite", and "NMC111" or "NMC811". These parameters correspond to cell content of recycled Li_2CO_3/LiOH, graphite, and NMC111/NMC811 hydroxide. In addition, parameter "ESLR" represents the share of enhanced pyrometallurgy within the overall pyrometallurgical recycling processes. Given that Li and graphite recovery exclusively occurs through enhanced pyrometallurgy, cells sourcing their recycled content from pyrometallurgical processes will exhibit a reduced net recycled content of Li and graphite compared to cells that source their recycled content from hydrometallurgical recycling processes.

2.3.3. Method for assessing inter-cell chemistry recycling

The methodology employed in this study includes an assessment of inter-cell chemistry recycling. This process entails recovering materials from outdated cell chemistries to potentially manufacture new cell chemistries, which may differ in their bill of materials and may not replicate the original cell chemistry. Therefore, the parameterized LCIs model NMC111 and NMC811 cells to potentially contain recycled materials sourced from both cell chemistries, reflecting the evolving practices in battery material recycling. Additionally, the supporting information S2 contains LCIs for recycled feedstock obtained through inter-cell chemistry recycling. A distinction between same-cell and inter-cell chemistry recycling is also incorporated into the model through the introduction of parameter "IRC".

2.3.4. Allocation of recycling process impacts to the recycled feedstock

According to the ISO 14041 standard, the environmental impacts of the recycling process should be divided among the recycled products through strategies such as sub-division and system expansion (Frischknecht, 2000). This should be done prior to allocation based on physical relationships or the economic value of the products. Although sub-division is the preferred strategy for dealing with joint production, it can be difficult to implement in some stages, such as thermal and mechanical pretreatment. Additionally, using system expansion is challenging and difficult to apply, as this study already takes into account multiple primary production pathways for each battery raw material, in addition to the recycling routes.

To assess the impact of the allocation method adopted, this study compares two allocation strategies to handle joint production in LIB recycling. The first strategy is based on the physical relationships between the inputs and product fractions of the recycling process, and the second strategy is based on the economic value of the products. The first proposed allocation strategy is based on the final mass of elements recovered in their respective product fraction, and allocates the preprocessing steps accordingly. Additionally, the impact of recovery processes dedicated solely to a particular element, such as flotation for graphite and early-stage lithium recovery for Li, are fully allocated to the recovered element. Furthermore, the impacts of deep recovery processes, such as acid leaching, solvent extraction, and matte refining, are allocated based on the input mole fraction of the specific element present in the black mass. This is because the amount of chemicals required for acid leaching depends on the chemical black mass composition and its pre-treatment steps. The amount of chemicals for solvent extraction and coprecipitation reactions is also directly proportional to the number of moles of transition metals present in the leaching solution as shown in the equations below from the studies of (Benjamasutin & Promphan, 2020; Stefaniak et al., 2020; Van Bommel & Dahn, 2009).

$$\textbf{\textit{Leaching}}: 2LiCoO_2 + 3H_2SO_4 + H_2O_2 \rightarrow 2CoSO_4 + Li_2SO_4 + 4H_2O + O_2$$

$$\textbf{\textit{Solvent extraction}}: Co^{2+}{}_{(aq)} + 2(R_2P(O)OH)_{(org)} \leftrightarrows Co[R_2P(O)O]_{2(org)} + 2H^+{}_{(aq)}$$

$$\textbf{\textit{Co - precipitation}}: Co^{2+} + nNH_3 \rightarrow \left[Co(NH_3)_n\right]^{2+}$$

$$\left[Co(NH_3)_n\right]^{2+} + 2OH^- \rightarrow Co(OH)_2 + nNH_3$$

However, chemicals which are dedicated solely to a particular element, such as $KMnO_4$ for Mn recovery, are fully allocated to the recovered element. It should be noted that there are many different options for solvent extraction and recovery for each element, involving various organic solvents and complex processes. Therefore, this study focuses on one representative option for each element.

The second allocation strategy allocates the impact of the entire recycling process based on the economic value of the products. It takes into account price volatility as a metric for economic evaluation. This is calculated by determining the average of the moving standard deviation (1981–2018) of USGS metal prices, using a seven-year time frame. This approach is based on the recommendations made in the study by (Renner & Wellmer, 2020). This provides a balanced view of the price fluctuations over time, determines the cost-effectiveness and economic viability of the recycling process, and identifies which recycled raw materials are the most price-volatile and thus require special attention. The LCI data for the recycled LIB raw materials are provided in supporting information S2.

2.4. Analysis of sensitivity and importance of LIB raw materials

One of the main goals of carrying out a sensitivity analysis in LCA studies is to test the robustness of allocation approaches and parameter values (Guo & Murphy, 2012). Sensitivity analysis methods can be classified as local or global. Local methods evaluate the change in model output value (GWP impact) based on a small uncertainty range of input parameters, while global methods evaluate the uncertainty of the output value over the whole range of uncertainty of input parameters (Wei et al., 2015). In general, global sensitivity analysis methods are preferred to estimate the uncertainty of the model output (Xu & Gertner, 2011). For this reason, global sensitivity analysis methods are used to assess the significance of different raw material supply routes in terms of their impact on CO_2 equivalent (eq.) emissions during the production of new LIB cells through a systematic mathematical approach.

The first method used is the variance-based Sobol sensitivity analysis method which estimates the contribution of each model parameter to the variance in the model output using ANOVA (Analysis Of Variances) decomposition (Sobol, 2001). The Sobol method is performed using the Python library OpenTURNS (Baudin et al., 2015). The output from the Sobol method includes the first-order indices (SF) and total-order indices (ST) of input parameters. The SF indices represent the influence of each input parameter on the model output when varied on its own, while the ST indices measure the influence of each input parameter on the model output in addition to its interactions with other input parameters. Furthermore, if the difference between SF and ST is large, it means that the parameter has strong interactions with other parameters, and that the effect on the output cannot be fully explained by its first-order effect.

The second method used in this study is the screening Morris method (MM) by (Morris, 1991). Unlike the Sobol method, the MM is computationally efficient and can analyze a large number of parameters (Sepulveda et al., 2013). This method uses a one-factor-at-a-time approach to deliver the average (μ), absolute average (μ*) and standard deviation values of the incremental ratio distribution, which represents the distribution of all variations in model output values between two points in input space. μ can be a negative value if the parameter has a negative correlation with the output. However, μ* is always positive and a large difference between μ and μ* suggests that the parameter has both positive and negative effects on the output, and its effect is not necessarily monotonic (Campolongo et al., 2007). The MM is performed using the Python library SALib (Herman & Usher, 2017).

In addition, the study uses random forest regression (RFR), a machine learning algorithm, to confirm the findings of sensitivity analysis methods. RFR has the advantage of being able to handle high-dimensional data (Rodriguez-Galiano et al., 2015), by using decision trees to classify variables. This study employs the random forest regressor ensemble from the Python library scikit-learn (Pedregosa et al., 2011). The relative importance of an input parameter to the model output is determined by the output of this regressor. Furthermore, for all sensitivity analysis methods, the number of Monte Carlo iterations was determined based on a ratio of 25 between the number of model evaluations and (model input parameters + 1). The triangular distributions listed in Table 1 are used to describe the uncertainty of modelling parameters. A minimum value of 0 % and a maximum value of 100 % are assumed for all distributions.

3. Results

3.1. Recycling routes

In this study, the GWP impacts of recycling routes and recycled raw materials for LIB production are investigated and compared to primary production. The results, as shown in Fig. 3, indicate that the environmental footprint of recycling waste LIBs can range from 17.8 to 21.5 kg CO_2 eq. per kWh battery pack. This is 30 % higher than the results from a recent publication by (Blömeke et al., 2022) that had recycling routes similar to the ones investigated in this study. The differences can be attributed to the different methodologies used in the studies, including the bottom-up vs. top-down LCI development approaches, landfilling vs. hydrometallurgical processing of slag, and extraction techniques for Mn and Li.

Pyrometallurgical recycling routes may have a higher impact than the hydrometallurgical route due to increased energy consumption by the smelting process and higher direct gaseous emissions. Similarly, the enhanced pyrometallurgical recycling route is found to be slightly advantageous than conventional pyrometallurgy. Reason for this is that a significant fraction of battery mass (Li and graphite) is removed in the preprocessing steps, reducing the impact of the smelting and matte refining processes. Inter-cell chemistry pyrometallurgical recycling of waste LIBs results in the highest environmental impact due to the impacts of smelting and matte refining in addition to the significant amounts of $NiSO_4$ and $CoSO_4$ needed to adjust the molar ratio of NMC hydroxides, as well as the increased co-precipitation process demand for NaOH, deionized water, and ammonia.

NaOH is likely the biggest driver of GWP impacts in all recycling routes due to the upstream energy-intensive chlor-alkali production process. This finding is consistent with previous studies, such as (Rinne et al., 2021; Blömeke et al., 2022). Direct CO_2 emissions and energy consumption are main drivers of GWP impacts in pyrometallurgical routes, whereas organic solvents, hydrogen peroxide and Na_2CO_3 are main drivers in the hydrometallurgical route.

3.2. Raw materials: primary and secondary supply routes

There is significant variability in CO_2 emissions across all raw materials, as indicated in Fig. 4. The primary supply with the highest GWP impacts for battery raw materials are $CoSO_4$ production from land mining of Ni and Cu ores, $NiSO_4$ production from laterite ores, and to a lesser extent battery-grade graphite production from natural graphite. Additionally, the GWP impacts from both primary and secondary supply routes of $CoSO_4$ and $NiSO_4$ show the widest range, reaching 20.7 and 17.4 kg CO_2 eq./kg, respectively. Moreover, $MnSO_4$ primary production through electrolytic processing routes is approximately six times more impactful than the chemical routes from the Ecoinvent database. This disparity is mainly attributed to the high electricity demand of the electrolysis process, assuming that it is supplied by the average electricity mix from the Chinese State Grid Corporation.

The use of different allocation strategies strongly determines the environmental burdens of recycled raw materials. For Li_2CO_3, the

Table 1
The parameters used in the LCIs of this study and their uncertainty distributions.

Parameter	Symbol	Distribution type	Mode value	Reference
Recycled Li_2CO_3 or LiOH content	li	Triangular	12.6 %	(Abdelbaky et al., 2021)
Recycled $NiSO_4$ content	ni	Triangular	32.3 %	(Abdelbaky et al., 2021)
Recycled $CoSO_4$ content	co	Triangular	57.3 %	(Abdelbaky et al., 2021)
Recycled $MnSO_4$ content	mn	Triangular	57.3 %	Same values as parameter (co) as they have the same molar ratio in NMC111 & NM811 cells and Mn was not in the scope of the reference study
Recycled graphite content	graphite	Triangular	34.2 %	(Abdelbaky et al., 2021)
Recycled NMC111 hydroxide content	NMC111	Triangular	49.0 %	Weighted average of recycled Ni, Co, & Mn content
Recycled NMC811 hydroxide content	NMC811	Triangular	37.3 %	Weighted average of recycled Ni, Co, & Mn content
Enhanced pyrometallurgy	ESLR	Uniform	50 %	Uniform probability for performing enhanced and conventional pyrometallurgy
Inter-cell recycling from NMC111 ⟶ NMC811	ICR_111_811	Triangular	100 %	100 % mode value for the triangular distribution as NMC811 is the novel cell chemistry and NMC111 will be more prevalent in the waste stream
Inter-cell recycling from NMC811 ⟶ NMC111	ICR_811_111	Triangular	0 %	0 % mode value because of the justification provided above
Primary Li_2CO_3 from spodumene	spod	Triangular	67 %	
Primary Li_2CO_3 from brines	1-spod	Triangular	33 %	No exact figures are available, but based on production of Argentina and Chile (U.S. Geological Survey, 2022)
Primary $NiSO_4$ from class 1 nickel	A_Ni	Triangular	0.9 %	(Lennon, 2021; U.S. Geological Survey, 2022)
Primary $NiSO_4$ from Cobalt institute LCI	B_Ni	Triangular	8.8 %	(Lennon, 2021; U.S. Geological Survey, 2022)
Primary $NiSO_4$ from molten ferronickel conversion	C_Ni	Triangular	64.5 %	(Lennon, 2021; U.S. Geological Survey, 2022)
Primary $NiSO_4$ from HPAL	D_Ni	Triangular	21.5 %	(Lennon, 2021; U.S. Geological Survey, 2022)
Primary $NiSO_4$ from PM nodules	E_Ni	Triangular	4.3 %	(Lennon, 2021; U.S. Geological Survey, 2022; Paulikas et al., 2020)
Primary $CoSO_4$ from Cobalt institute LCI	Land_Co	Triangular	96.6 %	
Primary $CoSO_4$ from PM nodules	1- Land_Co	Triangular	3.4 %	(U.S. Geological Survey, 2022; Paulikas et al., 2020)
Primary $MnSO_4$ from chemical Mn dioxide	A_Mn	Triangular	0 %	Assumed low probability since it is not representative of actual refining steps needed to produce battery-grade $MnSO_4$
Primary $MnSO_4$ from Mn concentrate	B_Mn	Triangular	0 %	Assumed low probability since it is not representative of actual refining steps needed to produce battery-grade $MnSO_4$
Primary $MnSO_4$ from EMM	C_Mn	Triangular	17 %	(Euro manganese Inc., 2019; Flook, 2019)
Primary $MnSO_4$ from EMD	D_Mn	Triangular	76 %	(Euro manganese Inc., 2019; Flook, 2019)
Primary $MnSO_4$ from PM nodules	E_Mn	Triangular	7 %	(U.S. Geological Survey, 2022; Paulikas et al., 2020)
Battery-grade natural graphite	nat_gr	Triangular	13 %	(Rystad Energy, 2022)
Battery-grade synthetic graphite	1-nat_gr	Triangular	87 %	(Rystad Energy, 2022)

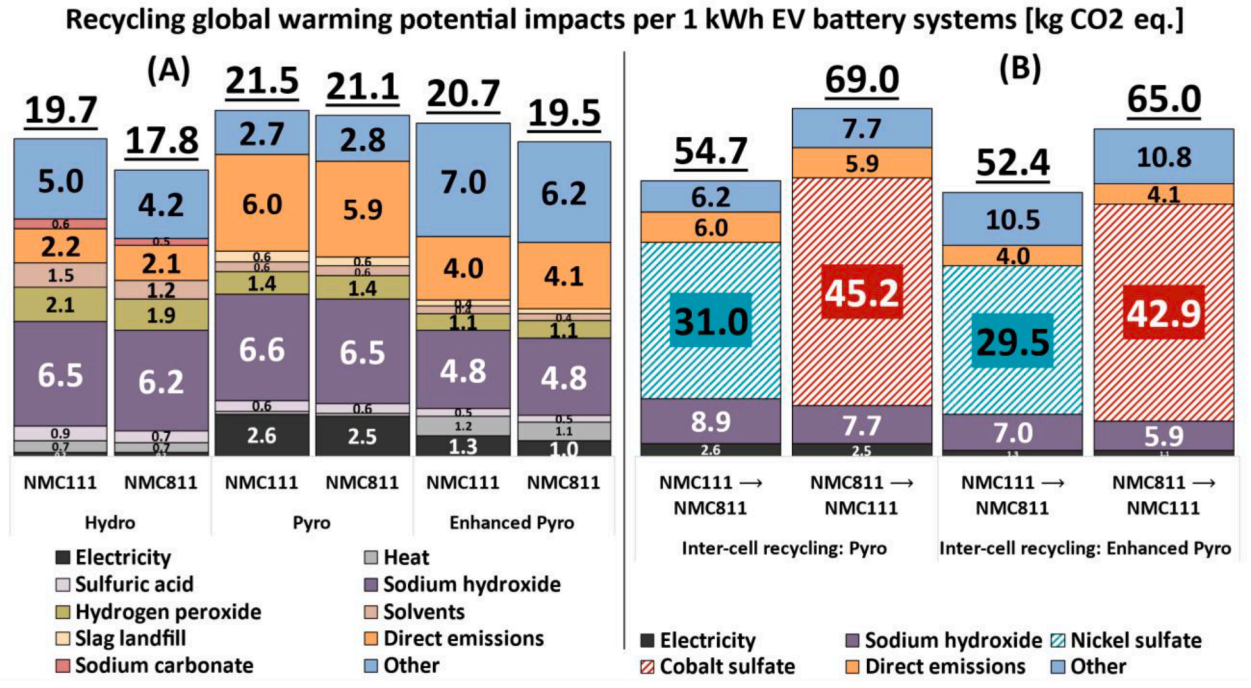

Fig. 3. GWP impacts of recycling and inter-cell recycling1 kWh battery packs using hydrometallurgical and pyrometallurgical processes. (A) shows the impacts of hydrometallurgical and pyrometallurgical recycling, with stacked bars indicating the main drivers of each process. (B) shows the impacts of inter-cell recycling using pyrometallurgical processes, with stacked bars indicating the main drivers of each process.

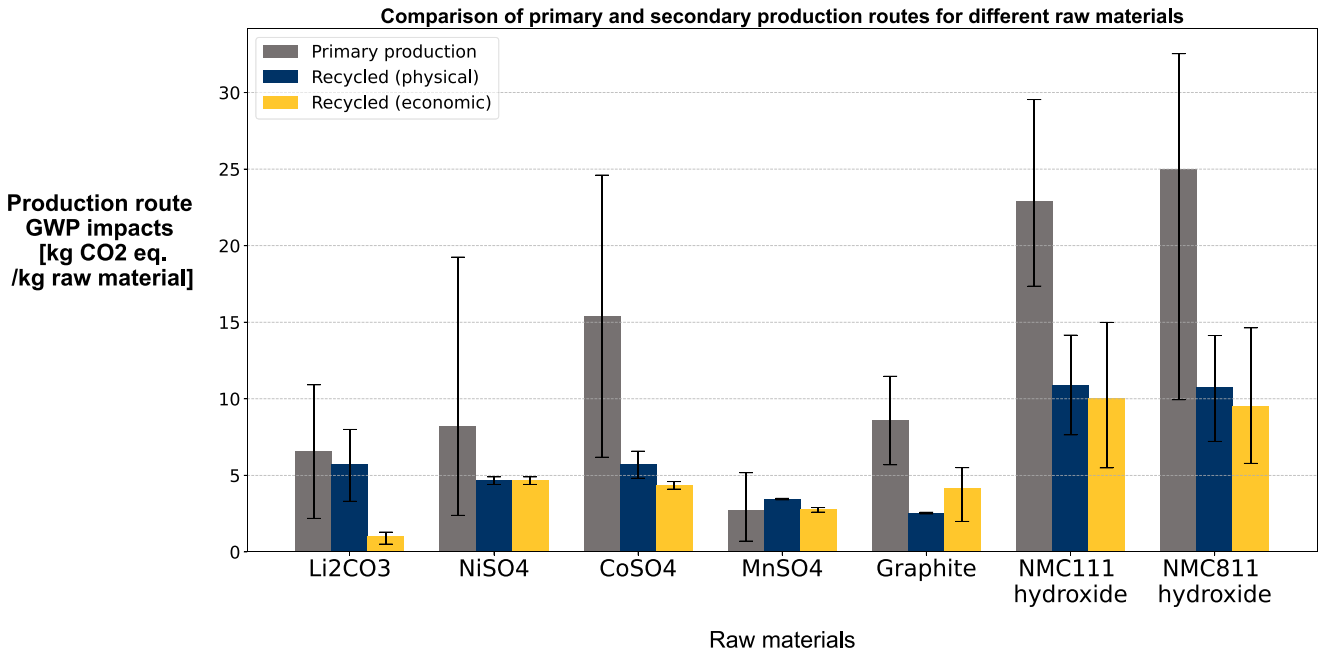

Fig. 4. The GWP scores of primary and secondary supply of LIB raw materials.

estimated environmental burdens using economic allocation are 40 % lower than specific physical allocation. However, it is important to note that this analysis did not include recent price spikes in the market price of Li_2CO_3, as more recent USGS price estimates are not yet available. Likewise, economic allocation factors assign a higher environmental burden to recycled graphite than physical allocation factors, given the relatively high market price of graphite. Recycled NMC hydroxides are likely to have lower environmental burdens than those from virgin raw materials. Roughly 30 % of the GWP burdens from the physical allocation method are attributed to NaOH required for co-precipitation in the matte refining process, while 10 % of the burdens are due to the energy consumption of the smelting process. Due to the absence of data on the recent price spikes in LIB raw materials, the physical allocation factors are applied to the recycled feedstock to derive the results in the upcoming sections. The use of economic allocation factors can be expanded upon in future research endeavors, because otherwise they will affect the representativeness of the results.

3.3. LIB cell production

For NMC111 cells, the estimated GWP impact of cell production is 93.2 kg CO_2 eq./kWh, considering 100 % primary production of the 5 battery raw materials considered in this study and using the mean values from the parameter distributions listed in Table 1. When recycled feedstock from hydrometallurgical recycling is used in cell production, this value decreases to 71.4 kg CO_2 eq./kWh, compared to 63.7 kg CO_2 eq./kWh with feedstock from pyrometallurgical recycling. On the one hand, the recycled feedstock from pyrometallurgical recycling results in a lower GWP for cell production as the main recycling product is NMC111 hydroxide, which can directly react with Li_2CO_3 to produce cathode active material. On the other hand, sulfate salts from hydrometallurgical recycling need to go through co-precipitation to yield NMC hydroxide that reacts with Li_2CO_3. For NMC811 cells, the GWP for cell production is 85.3 kg CO_2 eq./kWh when using primary production of the 5 raw materials, 67.7 kg CO_2 eq./kWh when using recycled feedstock from hydrometallurgical recycling, and 60 kg CO_2 eq./kWh with feedstock from pyrometallurgical recycling.

As discussed earlier in section 2, the supply chain of battery raw materials is dynamic. Consequently, the contribution of different primary and secondary supply routes will vary among battery producers based on several factors, such as future battery recycling volumes and the scaling up of different primary production and recycling processes. Therefore, performing a Monte Carlo simulation using the full uncertainty range of model parameters will aid in comprehending the complete range of potential GWP for cell production. As shown in Fig. 5, the developed LCA model estimates the mean GWP impact of producing 1 kWh NMC111 cells for closed-loop pyro- and hydrometallurgical recycled feedstock respectively, at 81.7 and 86.5 kg CO_2 eq., with a standard deviation of 5.7 and 4.5 kg CO_2-eq. Similarly, the production of 1 kWh NMC811 cells is estimated to have an average GWP impact of 79.1 and 77.4 kg CO_2 eq., with a standard deviation of 4.5 and 3.5 kg CO_2 eq. These results indicate substantial variability in the environmental performance of cell production, which can be attributed to the choice of primary and secondary supply routes of battery raw materials.

3.4. Global sensitivity analysis of cell production GWP

For NMC111 cells, RFR and Sobol scores in Table 2 demonstrate a high degree of agreement in terms of the ranking of most influential parameters. Both methods identify the most influential parameters to be:

1. The cell content of the recycled feedstock NMC111 hydroxide from the pyrometallurgical recycling routes.
2. The cell content of primary supply of $CoSO_4$ and Li_2CO_3 from spodumene.
3. The cell content of recycled $NiSO_4$, graphite and Li_2CO_3 feedstock from the hydrometallurgical recycling route.

The high Ni content in NMC811 cells highlights the significance of recycled $NiSO_4$ and recycled NMC811 hydroxide contents on cell production GWP. This is evident from the high scores of parameters “ni” and “NMC811” that are listed in Table 3. Additionally, parameter “C_Ni” has high importance scores being the primary supply route for $NiSO_4$ with the highest GHG emissions. The lower Co content in NMC811 cells implies that parameters associated with graphite content, i.e. “graphite” and “nat_gr”, and Li content, “spod”, will strongly influence the GWP impacts of NMC811 cell production.

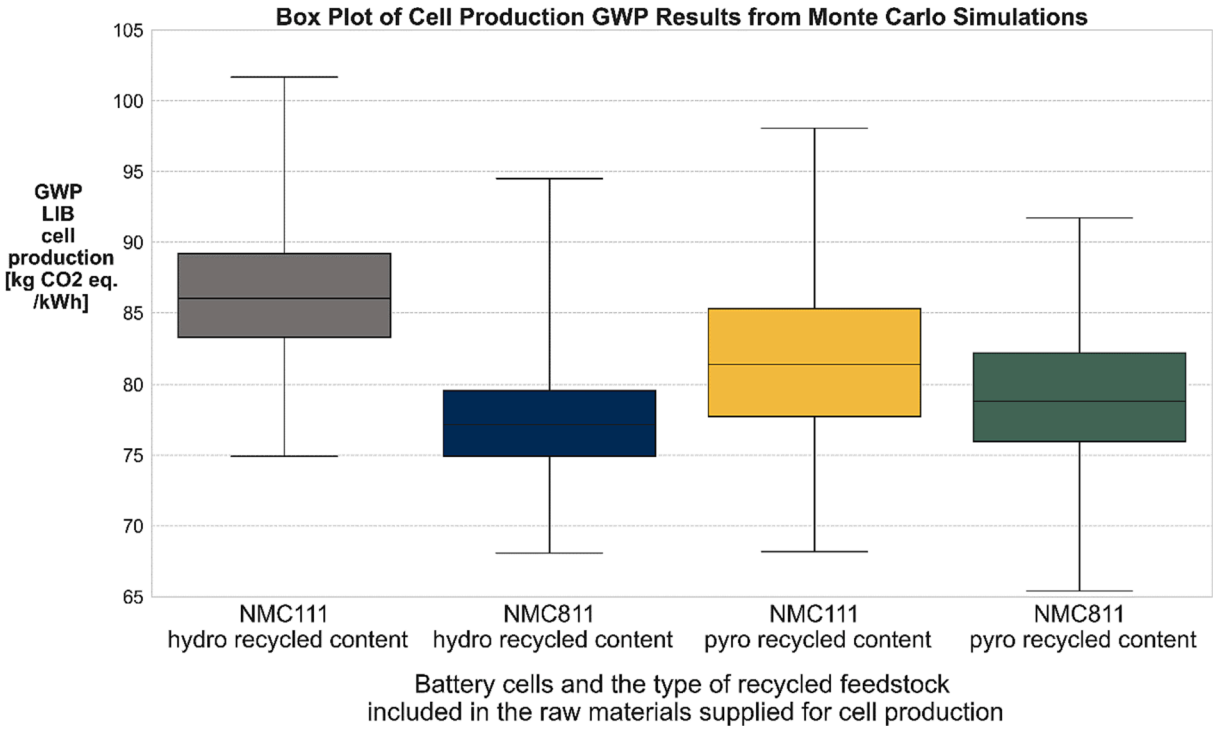

Fig. 5. The GWP impact of LIB cell production with recycled feedstocks from different recycling processes.

Table 2
Shortlist of most influential primary and secondary raw material supply routes for NMC111 cell production as determined by sensitivity analysis methods.

	RFR		MM				Sobol			
	Importance Score		μ		μ*		SF [%]		ST [%]	
Parameter Name	hydro	Pyro	hydro	Pyro	hydro	Pyro	hydro	Pyro	hydro	Pyro
NMC111		58.6 %		−21		21		57.1 %		59.3 %
land_Co	36.6 %	25.6 %	15	14	15	14	34.4 %	21.3 %	37.7 %	23.1 %
ni	7.8 %		−5		5		4.0 %		7.1 %	
graphite	5.9 %	0.8 %	−9	−4	9	4	7.2 %	1.5 %	14.9 %	1.8 %
li	5.7 %	0.7 %	−5	−2	5	3	3.1 %	0.3 %	10.3 %	0.5 %
spod	5.6 %	2.8 %	6	7	6	7	3.8 %	5.2 %	6.4 %	5.4 %
C_ni	4.3 %	1.6 %	4	6	4	6	5.1 %	2.6 %	7.9 %	2.9 %
ICR_811_111	1.8 %	0.9 %	1	0	1	2	0.0 %	0.2 %	1.9 %	0.5 %
Sum	**67.7 %**	**91.0 %**					**57.6 %**	**88.2 %**	**86.3 %**	**93.5 %**

Table 3
Shortlist of most influential primary and secondary raw material supply routes for NMC811 cell production as determined by sensitivity analysis methods.

	RFR		MM				Sobol			
	Importance Score		μ		μ*		SF [%]		ST [%]	
Parameter Name	hydro	Pyro	hydro	Pyro	hydro	Pyro	hydro	Pyro	hydro	Pyro
ni	33.9 %		−10		11		28.5 %		33.5 %	
C_ni	22.0 %	30.0 %	8	13	8	13	22.1 %	25.9 %	25.9 %	26.8 %
NMC811		27.0 %		−13		13		25.2 %		27.0 %
graphite	8.3 %	1.3 %	−9	−4	9	4	11.7 %	1.4 %	13.1 %	1.9 %
E_ni	7.7 %	6.9 %	−4	−6	4	6	6.2 %	9.4 %	7.7 %	10.3 %
ICR_111_811	1.0 %	6.1 %	0	3	1	3	0.3 %	9.7 %	0.6 %	11.2 %
spod	5.4 %	5.6 %	5	6	5	6	5.6 %	5.1 %	6.6 %	5.3 %
nat_gr	3.7 %	3.9 %	4	6	4	6	4.2 %	4.5 %	5.1 %	4.7 %
Sum	**82.0 %**	**80.7 %**					**78.5 %**	**81.2 %**	**92.5 %**	**87.2 %**

4. Discussion

4.1. Interpretation of sensitivity analysis results

Analyzing the μ values of the MM analysis, it becomes apparent that recycled NMC hydroxides have stronger negative correlations with cell production GWP than sulfate salts. This positions them as a more sustainable recycled feedstock due to their later entry point in cell manufacturing. Moreover, the high μ values (-4 and-9) for recycled graphite in Tables 2 and 3 suggest its potential in reducing cell production GWP. However, the anticipated surge in graphite demand within the European EV sector as anode active material for various cell

chemistries beyond NMC, such as lithium iron phosphate and Co-free Li-rich layered oxides, limits the capacity of recycled material to meet this demand. As a result, recycled graphite receives lower rankings in the RFR and Sobol methods when compared to recycled $NiSO_4$. Inter-cell chemistry recycling has a moderate positive correlation with cell production GWP, as indicated by the SF scores and positive μ values. Parameters relating to the cell content of recycled $NiSO_4$, $Li2CO_3$/LiOH, and graphite demonstrate significant interaction effects, apparent from both the SF and ST scores. These parameters also play a crucial role in determining the content of raw materials from primary supply routes.

The shift towards cathode materials rich in Ni and low in Co amplifies the impact of $NiSO_4$ primary and secondary supply routes on cell production GWP, while diminishing the influence of $CoSO_4$ supply routes. In Table 3, the parameter "C_ni" has a high rank in all sensitivity analysis methods, notably featuring high positive μ values (8 and 13) in the MM analysis. Moreover, the wide range of GHG emissions across $NiSO_4$ primary production routes, combined with the anticipated large market share of laterite ores in future Ni supply (which tend to have higher GHG emissions), emphasizes the significance of low GHG emission primary supply routes in cell production GWP. This significance is underscored by the high importance score of parameter "E_ni," which also has negative μ values (−4 and −6) in the MM analysis.

4.2. The effectiveness of recycled content targets in reducing the GWP of cell production

Expanding upon the new EU battery regulation targets for minimum recycled content in new batteries, this study employs the described methodology to evaluate the primary raw material supply routes that exert the most significant influence on the GWP of NMC811 cell production. The mode values of the triangular distributions used in the analysis for parameters "li", "ni", and "co" are replaced with the recycled content targets specified in the regulation for the year 2036. Notably, the regulation sets no targets for either graphite or Mn. In contrast, the findings of this study underscore the importance of primary supply routes for battery-grade graphite due to the notable disparity in GWP impacts observed between natural and synthetic graphite sources. Therefore, value 0 is assumed for parameters "mn" and "graphite".

Examining Fig. 6, the small variation in the mean GWP impacts of producing new NMC811 cells using different estimates for recycled content indicates the intricate challenge of achieving significant GWP reductions through recycled content alone, given the heightened influence of primary supply routes when the circularity gap remains open. Therefore, the establishment of targets for minimum recycled content in new batteries should be complemented by a suite of other strategies, which encompass sustainable sourcing of primary raw materials, using low-carbon energy supply in cell manufacturing (Lai et al., 2022; Xu et al., 2022), as well as optimizing the entire supply chain. Additionally, the importance scores in Table 4 indicate that the absence of specific targets for recycled graphite leads to a greater influence of battery-grade graphite primary supply routes on cell production GWP. Similarly, the lower targets set in the regulation for recycled Ni and Co content in new batteries than those assumed in this study lead to greater influence of $NiSO_4$ and $CoSO_4$ primary supply routes.

Table 4
Recalculated RFR importance scores for GWP impacts of NMC811 cell production with recycled feedstock from hydrometallurgical recycling processes.

	This study	EU regulation recycled content targets
Parameter Name	**Importance Score**	
nat_gr	3.7 %	10.3 %
li	1.7 %	1.4 %
spod	5.4 %	4.8 %
ni	33.9 %	31.1 %
A_ni + B_ni + C_ni + D_ni + E_ni	36.5 %	40.0 %
co	0.9 %	2.6 %
Land_Co	2.2 %	3.3 %
A_mn + B_mn + C_mn + D_mn + E_mn	5.2 %	5.2 %
ICR	1.0 %	1.3 %

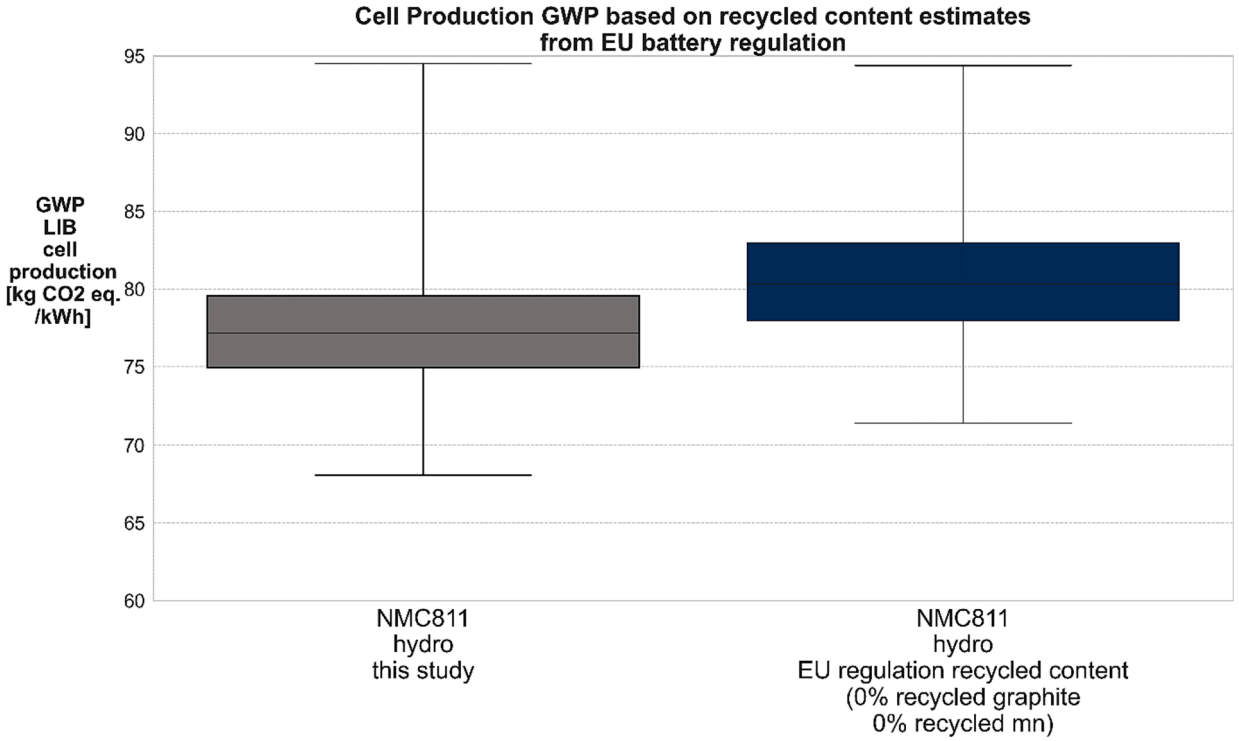

Fig. 6. The GWP impact of NMC811 cell production with recycled content targets set in the EU battery regulation.

4.3. Limitations and future research

The study has several limitations that could be addressed by future research. The first limitation is that GWP is just one aspect of the full environmental impacts of cell production, and other impact categories may have different drivers. For example, in water depletion, hydrometallurgical recycling may be more impactful than pyrometallurgical recycling, and Li_2CO_3 production from brine can be more impactful than spodumene. The second limitation is that the study did not analyze the environmental impacts of hydrometallurgical processing of slag from pyrometallurgical recycling. However, the study's findings support those of (Blömeke et al., 2022) that hydrometallurgical treatment of slags will result in additional recovery of Li and Mn, while it can be expected to go along with higher energy and chemicals demands than early-stage lithium recovery. Hydrometallurgical processing of slag could reduce the economic and environmental benefits of pyrometallurgical recycling (Blömeke et al., 2022), but further research is needed to fully understand its potential benefits and drawbacks on cell production. The third limitation of the study is its focus on representative pyrometallurgical and hydrometallurgical recycling processes, while in reality, there are numerous extraction methods, each with the potential to significantly influence the outcomes of the LCA model and, in particular, the sensitivity analysis. The fourth limitation is that although the focus was on recycling processes, additional primary supply routes and battery raw materials could be included in the analysis; i.e. Al and Cu. Therefore, future work can expand on primary supply routes, and include aspects such as regionalized production (Schenker et al., 2022), ore grade decline (Manjong et al., 2021), metal extraction rate during smelting, and optimized cell production to better understand the GWP impacts of LIB cell production.

Declaration of generative AI and AI-assisted technologies in the writing process

During the preparation of this work, the first author used ChatGPT in order to improve the use of English language in the first draft of this manuscript and developing python scripts for some of the figures used. After using this tool/service, the authors reviewed and edited the content as needed and take full responsibility for the content of the publication.

CRediT authorship contribution statement

Mohammad Abdelbaky: Methodology, Software, Writing – original draft, Writing – review & editing. **Lilian Schwich:** Formal analysis, Methodology, Resources, Validation, Writing – review & editing. **João Henriques:** Formal analysis, Software. **Bernd Friedrich:** Supervision, Validation, Writing – review & editing. **Jef R. Peeters:** Conceptualization, Formal analysis, Project administration, Supervision, Validation, Writing – review & editing. **Wim Dewulf:** Conceptualization, Formal analysis, Funding acquisition, Supervision, Validation, Writing – review & editing.

Declaration of Competing Interest

The authors declare the following financial interests/personal relationships which may be considered as potential competing interests: Lilian Schwich reports a relationship with cylib GmbH that includes: board membership. Lilian is the CEO of battery recycling company cylib GmbH. The co-author has contributed to this work as a researcher at the IME Institute in the context of the European Horizon 2020 project Si-drive which started in 2019.

Data availability

Data used in this research is available in the supplementary information

Acknowledgments

The authors would like to extend their thanks to Paul Sabarny, Eleonora Crenna, Roland Hischier, Karel van Acker, Gwendolyn Bailey, and Antoine Beylot for their valuable feedback throughout the long process of preparing this article.

Funding information

The authors would like to acknowledge funding from the European Union's Horizon 2020 research and innovation programme Si-DRIVE project under Grant Agreement No. 814464.

Appendix A. Supplementary data

Supplementary data to this article can be found online at https://doi.org/10.1016/j.clscn.2023.100130.

References

Abdelbaky, M., Peeters, J., Dewulf, W., 2021. On the influence of second use, future battery technologies, and battery lifetime on the maximum recycled content of future electric vehicle batteries in Europe. Waste Manag. 125, 1–9. https://doi.org/10.1016/j.wasman.2021.02.032.

Abdelbaky, M., Peeters, J., Van den Eynde, S., Zaplana, I., Dewulf, W., 2022. A comparative assessment of resource-use criticality in advanced lithium-ion battery technologies. Procedia CIRP 105, 7–12. https://doi.org/10.1016/j.procir.2022.02.002.

Arvidsson, R., Chordia, M., Nordelöf, A., 2022. Quantifying the life-cycle health impacts of a cobalt-containing lithium-ion battery. Int. J. LCA 27, 1106–1118. https://doi.org/10.1007/s11367-022-02084-3.

Baudin, M., Dutfoy, A., Iooss, B., Popelin, A., 2015. OpenTURNS: An industrial software for uncertainty quantification in simulation. In: Ghanem, R., Higdon, D., Owhadi, H. (Eds.), Handbook of Uncertainty Quantification. Springer, Cham. https://doi.org/10.1007/978-3-319-11259-6_64-1.

Benjamasutin, P., Promphan, R., 2020. Determination of optimal parameters for the application of hydrogen peroxide as reducing agent in the leaching process. Chalmers University Of Technology, Gothenburg, Sweden. Retrieved from https://odr.chalmers.se/server/api/core/bitstreams/8db14eef-f434-4899-b99f-b1b3fb676ec2/content.

Blömeke, S., Scheller, C., Cerdas, F., Thies, C., Hachenberger, R., Gonter, M., Spengler, T. S., 2022. Material and energy flow analysis for environmental and Economic Impact Assessment of industrial recycling routes for lithium-ion traction batteries. J. Clean. Prod. 377, 134344 https://doi.org/10.1016/j.jclepro.2022.134344.

Boubou, W., 2018. Manganese: No Longer Just an Input on Steel. Retrieved from The Assay: https://www.theassay.com/technology-metals-edition-insight/manganese-no-longer-just-an-input-on-steel/.

Bouter, A., Guichet, X., 2022. The greenhouse gas emissions of automotive lithium-ion batteries: a statistical review of life cycle assessment studies. J. Clean. Prod. 344, 130994 https://doi.org/10.1016/j.jclepro.2022.130994.

Campolongo, F., Cariboni, J., Saltelli, A., 2007. An effective screening design for sensitivity analysis of large models. Environ. Model. Softw. 22 (10), 1509–1518. https://doi.org/10.1016/j.envsoft.2006.10.004.

Chen, Q., Lai, X., Gu, H., Tang, X., Gao, F., Han, X., Zheng, Y., 2022. Investigating carbon footprint and carbon reduction potential using a cradle-to-cradle LCA approach on lithium-ion batteries for electric vehicles in China. J. Clean. Prod. 369, 133342 https://doi.org/10.1016/j.jclepro.2022.133342.

Cobalt Institute. (2016). The environmental performance of refined cobalt—Life cycle inventory and life cycle assessment of refined cobalt—Summary report. Cobalt Institute. Retrieved from https://www.cobaltinstitute.org/life-cycle-assessment.html.

Crenna, E., Gauch, M., Widmer, R., Wäger, P., Hischier, R., 2021. Towards more flexibility and transparency in life cycle inventories for Lithium-ion batteries. Resour. Conserv. Recycl. 170, 105619 https://doi.org/10.1016/j.resconrec.2021.105619.

Dai, Q., Spangenberger, J., Ahmed, S., Gaines, L., Kelly, J.C., Wang, M., 2019. EverBatt: A Closed-loop Battery Recycling Cost and Environmental Impacts Model. United States. https://doi.org/10.2172/1530874.

Dunn, J. B., James, C., Gaines, L., Gallagher, K., Dai, Q., & Kelly, J. C. (2015). *Material and Energy Flows in the Production of Cathode and Anode Materials for Lithium Ion Batteries.* United States: Argonne National Lab. (ANL), Argonne, IL (United States). https://doi.org/10.2172/1224963.

Engels, P., Cerdas, F., Dettmer, T., Frey, C., Hentschel, J., Herrmann, C., Schueler, M., 2022a. Life cycle assessment of natural graphite production for lithium-ion battery anodes based on Industrial Primary Data. J. Clean. Prod. 336, 130474 https://doi.org/10.1016/j.jclepro.2022.130474.

Engels, P., Kononova, N., Khalid, U., Cerdas, F., Herrmann, C., 2022b. Methodology for a combined uncertainty analysis and data quality rating of existing graphite datasets in context of battery lcas. Procedia CIRP 105, 577–582. https://doi.org/10.1016/j.procir.2022.02.096.

Euro manganese Inc, 2019. FOCUS ON GREEN AND EUROPEAN ULTRA HIGH-PURITY MANGANESE PRODUCTS. Retrieved from Asx: https://www.asx.com.au/asxpdf/20190916/pdf/448jvq94y3vfn0.pdf.

European Commission. (2019). *Delivering the European Green Deal*. Retrieved September 15, 2022, from https://ec.europa.eu/info/strategy/priorities-2019-2024/european-green-deal/delivering-european-green-deal_en.

European Commission. (2021). *'Fit for 55': delivering the EU's 2030 Climate Target on the way to climate neutrality*. Retrieved September 15, 2022, from https://eur-lex.europa.eu/legal-content/EN/TXT/HTML/?uri=CELEX:52021DC0550&from=EN.

European Commission. (2023). Proposal for a REGULATION OF THE EUROPEAN PARLIAMENT AND OF THE COUNCIL establishing a framework for ensuring a secure and sustainable supply of critical raw materials and amending Regulations (EU) 168/2013, (EU) 2018/858, 2018/1724 and (EU) 2019/1020. Brussels: EUR-Lex. Retrieved from https://eur-lex.europa.eu/legal-content/EN/TXT/?uri=CELEX%3A52023PC0160.

European Parliament. (2023). *REGULATION OF THE EUROPEAN PARLIAMENT AND OF THE COUNCIL concerning batteries and waste batteries, amending Directive 2008/98/EC and Regulation (EU) 2019/1020 and repealing Directive 2006/66/EC.* 2020/0353 (COD). Retrieved from https://data.consilium.europa.eu/doc/document/PE-2-2023-INIT/en/pdf.

Fazio, S., Biganzioli, F., De Laurentiis, V., Zampori, L., Sala, S., & Diaconu, E. (2018). *Supporting information to the characterisation factors of recommended EF Life Cycle Impact Assessment methods, version 2, from ILCD to EF 3.0, EUR 29600 EN*. Ispra: European Commission,. https://doi.org/10.2760/002447.

Flook, R., 2019. Manganese: the black art. Retrieved from Element 25: https://www.element25.com.au/site/PDF/1771_0/BenchmarkMineralIntelligenceManganeseTheBlackArt.

Frischknecht, R., 2000. Allocation in life cycle inventory analysis for joint production. Int. J. LCA 5, 85–95. https://doi.org/10.1007/BF02979729.

George, D.B., Nexhip, C., George-Kennedy, D., Foster, R., Walton, R., 2006. Copper Matte Granulation at The Kennecott Utah Copper Smelter. San Antonio, Texas, USA, Granulation Molten Materials, TMS.

GLAD. (2020). *manganese sulfate production, UPR, ecoinvent 3.6, Allocation, APOS*. Retrieved October 31, 2022, from The Global LCA Data Access network: https://www.globallcadataaccess.org/manganese-sulfate-production-upr-ecoinvent-36-allocation-apos.

Goldie-Scot, L., 2019. A Behind the Scenes Take on Lithium-ion Battery Prices. Retrieved from BloombergNEF: https://about.bnef.com/blog/behind-scenes-take-lithium-ion-battery-prices/.

Guo, M., Murphy, R., 2012. LCA data quality: Sensitivity and uncertainty analysis. Sci. Total Environ. 435, 230–243. https://doi.org/10.1016/j.scitotenv.2012.07.006.

Herman, J., Usher, W., 2017. SALib: An open-source Python library for sensitivity analysis. J. Open Source Software 2 (9). https://doi.org/10.21105/joss.00097.

Hischier, R., Hellweg, S., Capello, C., Primas, A., 2004. Establishing life cycle inventories of chemicals based on differing data availability (9 PP). Int. J. LCA 10 (1), 59–67. https://doi.org/10.1065/lca2004.10.181.7.

IEA. (2019). *Global EV Outlook 2019*. Paris: IEA. Retrieved from https://www.iea.org/reports/global-ev-outlook-2019.

IEA. (2023). *Global EV Outlook 2023*. Paris: IEA. Retrieved from https://www.iea.org/reports/global-ev-outlook-2023.

Jiang, S., Zhang, L., Li, F., Hua, H., Liu, X., Yuan, Z., Wu, H., 2020. Environmental impacts of lithium production showing the importance of primary data of upstream process in life-cycle assessment. J. Environ. Manage. 262, 110253 https://doi.org/10.1016/j.jenvman.2020.110253.

Jin, H., 2022. Analysis: Ukraine invasion sets back Musk's dream for cheaper EVs, for now. Retrieved from Reuters: https://www.reuters.com/technology/ukraine-invasion-sets-back-musks-dream-cheaper-evs-now-2022-03-07/.

Kesler, S., Gruber, P., Medina, P., Keoleian, G., Everson, M., Wallington, T., 2012. Global lithium resources: Relative importance of pegmatite, brine and other deposits. Ore Geol. Rev. 48, 55–69. https://doi.org/10.1016/j.oregeorev.2012.05.006.

Lai, X., Chen, Q., Tang, X., Zhou, Y., Gao, F., Guo, Y., Zheng, Y., 2022. Critical review of life cycle assessment of lithium-ion batteries for electric vehicles: a lifespan perspective. eTransportation 12, 100169. https://doi.org/10.1016/j.etran.2022.100169.

Lennon, J. (2021). The nickel market outlook: The hype vs. the reality. Presented at Benchmark's mineral intelligence seminar: EV Fest.

Lovins, A., 2022. Six Solutions to Battery Mineral Challenges. Retrieved from RMI: https://rmi.org/insight/six-solutions-to-battery-mineral-challenges/.

Ma, X., Chen, M., Chen, B., Meng, Z., Wang, Y., 2019. High-performance graphite recovered from spent lithium-ion batteries. ACS Sustainable Chem. Eng 7 (24), 19732–19738. https://doi.org/10.1021/acssuschemeng.9b05003.

Manjong, N., Usai, L., Burheim, O., Strømman, A., 2021. Life cycle modelling of extraction and processing of battery minerals—a parametric approach. Batteries 7 (3), 57. https://doi.org/10.3390/batteries7030057.

Moores, S., 2022. Raw materials & mining - the limiting factor in the energy storage revolution. Retrieved from Twitter: https://twitter.com/sdmoores/status/1551643670574669826.

Morgan, C., 2017. Resource Estimates of the Clarion-Clipperton Manganese Nodule Deposits. In: Cronan, I.D.S. (Ed.), Handbook of Marine Mineral Deposits. Routledge, New York, pp. 145–170. https://doi.org/10.1201/9780203752760.

Morris, M.D., 1991. Factorial sampling plans for preliminary computational experiments. Technometrics 33 (2), 161–174. https://doi.org/10.1080/00401706.1991.10484804.

Önal, M.A., Panda, L., Kopparthi, P., Singh, V., Venkatesan, P., Borra, C.R., 2021. Hydrometallurgical production of electrolytic manganese dioxide (EMD) from furnace fines. Minerals 11 (7). https://doi.org/10.3390/min11070712.

Paulikas, D., Katona, S., Ilves, E., Ali, S., 2020. Life cycle climate change impacts of producing battery metals from land ores versus deep-sea polymetallic nodules. J. Clean. Prod. 275, 123822 https://doi.org/10.1016/j.jclepro.2020.123822.

Pedregosa, F., Varoquaux, G., Gramfort, A., Michel, V., Thirion, B., Grisel, O., Duchesnay, E., 2011. Scikit-learn: Machine Learning in Python. JMLR 12, 2825–2830.

Pell, R., & Lindsay, J. (2022). *Comparative life cycle assessment study of solid state and lithium-ion batteries for electric vehicle application in Europe.* The European Federation for Transport and Environment. Retrieved from https://www.transportenvironment.org/wp-content/uploads/2022/07/2022_07_LCA_research_by_Minviro.pdf.

Pillot, C., 2021. EU battery demand and supply. Retrieved from Eurobat: https://www.eurobat.org/wp-content/uploads/2021/05/Avicenne_EU_Market_-_summary_110321.pdf.

Porzio, J., Scown, C., 2021. Life-Cycle Assessment Considerations for Batteries and Battery Materials. Adv. Energy Mater. 11 (33), 2100771. https://doi.org/10.1002/aenm.202100771.

Qiao, Q., Zhao, F., Liu, Z., Hao, H., 2019. Electric vehicle recycling in China: Economic and environmental benefits. Resour. Conserv. Recycl. 140, 45–53. https://doi.org/10.1016/j.resconrec.2018.09.003.

Renner, S., Wellmer, F., 2020. Volatility drivers on the metal market and exposure of producing countries. Miner Econ 33, 311–340. https://doi.org/10.1007/s13563-019-00200-8.

Rinne, M., Elomaa, H., Porvali, A., Lundström, M., 2021. Simulation-based Life Cycle Assessment for hydrometallurgical recycling of mixed Lib and nimh waste. Resour. Conserv. Recycl. 170, 105586 https://doi.org/10.1016/j.resconrec.2021.105586.

Rodriguez-Galiano, V., Sanchez-Castillo, M., Chica-Olmo, M., Chica-Rivas, M., 2015. Machine learning predictive models for mineral prospectivity: An evaluation of neural networks, random forest, regression trees and support vector machines. Ore Geol. Rev. 71, 804–818. https://doi.org/10.1016/j.oregeorev.2015.01.001.

Rystad Energy. (2022). *Fake it till you make it: Synthetic graphite holds the key to meeting battery demand surge, despite ESG concerns*. Retrieved from Rystad Energy: https://www.rystadenergy.com/news/fake-it-till-you-make-it-synthetic-graphite-holds-the-key-to-meeting-battery-dema.

Schenker, V., Oberschelp, C., Pfister, S., 2022. Regionalized life cycle assessment of present and future lithium production for Li-ion batteries. Resour. Conserv. Recycl. 187, 106611 https://doi.org/10.1016/j.resconrec.2022.106611.

Schwich, L., Schubert, T., Friedrich, B., 2021. Early-stage recovery of lithium from tailored thermal conditioned Black Mass Part I: Mobilizing lithium via supercritical CO2-Carbonation. Metals 11 (2), 177. https://doi.org/10.3390/met11020177.

Sepulveda, F.D., Cisternas, L.A., Gálvez, E.D., 2013. Global Sensitivity Analysis of a mineral processing flowsheet. Computer Aided Chemical Engineering 32, 913–918. https://doi.org/10.1016/b978-0-444-63234-0.50153-6.

Shah, A., 2022. Tata Motors says 20% rise in battery cell costs increasing short-term pressure. Retrieved from Reuters: https://www.reuters.com/business/autos-transportation/tata-motors-says-20-rise-battery-cell-costs-increasing-short-term-pressure-2022-03-29/#:~:text=NEW%20DELHI%2C%20March%2029%20(Reuters,. company%20in%20the%20short%2Dterm.

Sobol, I., 2001. Global sensitivity indices for nonlinear mathematical models and their Monte Carlo estimates. Math. Comput. Simul 55 (1–3), 271–280. https://doi.org/10.1016/S0378-4754(00)00270-6.

Sphera. (2021). *Summary Life Cycle Assessment Report: Nickel Sulphate Hexahydrate.* The Nickel Institute.

Stamp, A., Lang, D., Wäger, P., 2012. Environmental impacts of a transition toward e-mobility: the present and future role of lithium carbonate production. J. Clean. Prod. 23 (1), 104–112. https://doi.org/10.1016/j.jclepro.2011.10.026.

Stefaniak, J., Karwacka, S., Janiszewska, M., Dutta, A., Rene, E.R., Regel-Rosocka, M., 2020. Co(II) and ni(ii) transport from model and real sulfate solutions by extraction with bis(2,4,4-trimethylpentyl)phosphinic acid (Cyanex 272). Chemosphere 254, 126869. https://doi.org/10.1016/j.chemosphere.2020.126869.

Steubing, B., de Koning, D., Haas, A., Mutel, C.L., 2020. The Activity Browser — An open source LCA software building on top of the brightway framework. Software Impacts 3, 100012. https://doi.org/10.1016/j.simpa.2019.100012.

Tsuji, K., 2022. Global Value Chains: Graphite in Lithium-ion Batteries for Electric Vehicles. Retrieved from USITC: https://www.usitc.gov/publications/332/working_papers/gvc_paper.pdf.

Tytgat, J. (2022). The road to climate-neutral EV batteries: opportunities and regulatory framework. *Presented at LCE 2022 Conference*. Leuven, Belgium.

U.S. Geological Survey. (2022). *Mineral commodity summaries 2022*. U.S. Geological Survey. https://doi.org/10.3133/mcs2022.

U.S. Geological Survey. (2023). *Mineral commodity summaries 2023*. U.S. Geological Survey. https://doi.org/10.3133/mcs2023.

Van Bommel, A., Dahn, J., 2009. Analysis of the growth mechanism of coprecipitated spherical and dense nickel, manganese, and cobalt-containing hydroxides in the presence of aqueous ammonia. Chem. Mater. 21 (8), 1500–1503. https://doi.org/10.1021/cm803144d.

Wei, W., Larrey-Lassalle, P., Faure, T., Dumoulin, N., Roux, P., Mathias, J.-D., 2015. How to conduct a proper sensitivity analysis in life cycle assessment: Taking into account correlations within LCI data and interactions within the LCA calculation model. Environ. Sci. Technol. 49 (1), 377–385. https://doi.org/10.1021/es502128k.

Wernet, G., Bauer, C., Steubing, B., Reinhard, J., Moreno-Ruiz, E., Weidema, B., 2016. The ecoinvent database version 3 (part I): overview and methodology. Int. J. LCA 21 (9), 1218–1230. https://doi.org/10.1007/s11367-016-1087-8.

Windisch-Kern, S., Holzer, A., Ponak, C., Raupenstrauch, H., 2021. Pyrometallurgical lithium-ion-battery recycling: Approach to limiting lithium slagging with the indured reactor concept. Processes 9 (1), 84. https://doi.org/10.3390/pr9010084.

Xu, C., Gertner, G., 2011. Understanding and comparisons of different sampling approaches for the Fourier Amplitudes Sensitivity Test (FAST). Comput. Stat. Data Anal. 55 (1), 184–198. https://doi.org/10.1016/j.csda.2010.06.028.

Xu, C., Steubing, B., Hu, M., Harpprecht, C., van der Meide, M., Tukker, A., 2022. Future greenhouse gas emissions of automotive lithium-ion battery cell production. Resour. Conserv. Recycl. 187, 106606 https://doi.org/10.1016/j.resconrec.2022.106606.

Zhang, G., Du, Z., He, Y., Wang, H., Xie, W., Zhang, T., 2019a. A sustainable process for the recovery of anode and cathode materials derived from spent lithium-ion batteries. Sustainability 11 (8), 2363. https://doi.org/10.3390/su11082363.

Zhang, G., He, Y., Wang, H.F., Xie, W., Zhu, X., 2019b. Application of mechanical crushing combined with pyrolysis-enhanced flotation technology to recover graphite and licoo2 from spent lithium-ion batteries. J. Clean. Prod. 231, 1418–1427. https://doi.org/10.1016/j.jclepro.2019.04.279.

Zhang, J., Li, X., Song, D., Miao, Y., Song, J., Zhang, L., 2018. Effective regeneration of anode material recycled from scrapped Li-Ion Batteries. J. Power Sources 390, 38–44. https://doi.org/10.1016/j.jpowsour.2018.04.039.

Zhang, R., Ma, X., Shen, X., Zhai, Y., Zhang, T., Ji, C., Hong, J., 2020. Life cycle assessment of electrolytic manganese metal production. J. Clean. Prod. 253, 119951 https://doi.org/10.1016/j.jclepro.2019.119951.